Nonlinear images of scatterers in chirped pulsed laser beams*

Hu Yong-Hua(胡勇华), Wang You-Wen(王友文),
Wen Shuang-Chun(文双春)†, and Fan Dian-Yuan(范滇元)

School of Computer and Communication, Hunan University, Changsha 410082, *China*

(Received 24 November 2009; revised manuscript received 24 May 2010)

The bandwidth and the duration of incident pulsed beam are proved to play important roles in modifying the nonlinear image of amplitude-type scatterer. It is found that the initially positive chirp-type bandwidth can suppress the nonlinear image, while the negative one can enhance it, and that both effects are inversely proportional to the incident pulse duration. Numerical simulations further demonstrate that the location of nonlinear image is at the conjugate plane of the scatterer and that, for negatively pre-chirped pulsed beam, the nonlinear image peak intensity can be higher than that in the corresponding monochromatic case under certain conditions. Moreover the effect of group velocity dispersion on nonlinear image is found to be similar to that of chirp-type bandwidth.

Keywords: pulsed laser beam, nonlinear propagation, nonlinear image, self-focusing
PACC: 4260K, 4265

1. Introduction

In most high power laser systems, such as inertial confinement fusion (ICF) lasers, the beam uniformity is very important. However, scatterers, such as scratch, dirt, dust, bubbles, or even local imperfections in optical components cause amplitude and/or phase fluctuations in high-power laser beams, and thus decrease the beam uniformity and even damage expensive optical components by nonlinear effects. Two kinds of nonlinear effects related to such fluctuations are vital to high power laser systems. One is small-scale self-focusing;[1−8] the other is nonlinear formation of holographic image, which causes nonlinear image, also called as hot image.[9−16] There are inherent connections between them, for both of them result from the nonlinear polarization caused by the third order susceptibility $\chi^{(3)}$ of the nonlinear medium. Nonlinear image is a special case of self-focusing, or nonlinear refraction in a medium with an intensity-dependent index of refraction, yet it is not the direct result of small-scale self-focusing.[5−8] On the other hand, the propagation of high-power broadband beams has attracted intense attention from researchers working on ICF drivers for about two decades, since it has been recognized that using a beam with a certain quantity of bandwidth can achieve smoother, more uniform laser irradiance profiles at the target.[17−19] Though the underlying physical mechanism and the features of nonlinear image have been studied by many authors,[9−16] the influence of bandwidth and chirp on nonlinear image is not very clear.

This paper is devoted to the study on the nonlinear formation of holographic image in high-power broadband beams. The propagating process of nonlinear formation of holographic image is called imaging process. The remainder of the paper is organized as follows. In Section 2 the models are given. In Section 3 is presented the theoretical analysis on the imaging process in pulsed laser beams. In Section 4 are shown the main features of the nonlinear imaging by comparing them with those in the monochromatic beam case and presented the simulation results of the influence of bandwidth, temporal chirp, duration and group velocity dispersion (GVD) on nonlinear image. Finally, some conclusions drawn from the present study in Section 5.

2. Models

It is known that the envelope approximation is satisfied for pulses whose time durations are bigger than a single oscillating cycle. Under the envelope approximation and the scalar approximation, the electric field of the incident beam which propagates along the

*Project supported by the National Natural Science Foundation of China (Grant Nos. 60890202 and 10974049).
†Corresponding author. E-mail: scwen@vip.sina.com
© 2010 Chinese Physical Society and IOP Publishing Ltd

z axis can be written as

$$E(x,y,z,t) = A(x,y,z,t)\exp(-\mathrm{i}k_0 z), \quad (1)$$

where $A(x, y, z, t)$ is the envelope of the electric field, $k_0 = 2\pi n/\lambda_0$ is the wavenumber, n is the linear refractive index of medium, λ_0 is the pulse central wavelength in free space. We assume that the envelope of the incident field can be written as

$$A(0,r,\tau) = A_0 \exp\left(-\frac{1+\mathrm{i}C}{2}\frac{\tau^2}{\tau_0^2}\right)\exp\left[-\frac{1}{2}\left(\frac{r}{r_0}\right)^{2m}\right], \quad (2)$$

where A_0 is the peak amplitude, $r = (x^2+y^2)^{1/2}$, τ_0 and r_0 denote half the initial temporal width and half the initial spatial width at $1/e$-intensity point, respectively, $\tau = t - (z/v_\mathrm{g})$ is the relative time scale (with t being the real time and v_g the pulse group velocity), C is the initial temporal chirp and m is the super-Gaussian order. We set A_0 to be a fixed value in what follows for the sake of comparison.

The formation of nonlinear image in a pulsed laser beam is sketched in Fig. 1, where the imaging process is composed of two kinds of physical processes: the diffraction in free space and the nonlinear propagation in the nonlinear medium. The main difference from the monochromatic beam case is that the bandwidth will influence the propagation in the nonlinear medium through spatiotemporal interplay.

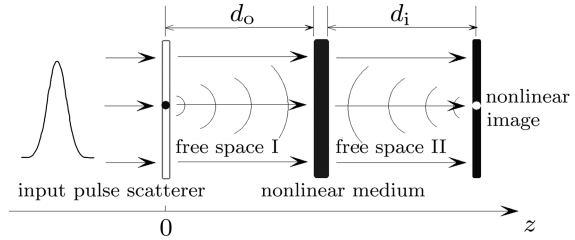


Fig. 1. Sketch map of imaging process in pulsed laser beam for an amplitude-type scatterer.

For simplicity, we assume that the first optical element, i.e., the scatterer, has a long straight scratch along the y axis and that the corresponding amplitude transmissivity distribution can be described as

$$T(x) = \begin{cases} \rho & \text{for} \quad |x| \le a_0/2, \\ 1 & \text{for} \quad |x| > a_0/2, \end{cases} \quad (3)$$

where a_0 is the transverse width of the scratch and ρ is a real number. Besides, the scatterer has no effect on the phase of the pulsed beam passing through it. We neglect all other effects and the thickness of the scatterer, and then the output field envelope of the scatterer can be written as

$$U_0(x_0,y_0,\tau) = A(0,x_0,y_0,\tau)\cdot T(x). \quad (4)$$

3. Theoretical analysis

For the pulsed beam propagation in free space I, only diffraction takes effect. Under the paraxial approximation, the envelope in the incident surface (x_1, y_1) of the nonlinear medium is given by the Fresnel diffraction integral as

$$U(d_1,x_1,y_1,\tau) = \int_{-\infty}^{\infty}\left\{\frac{\omega}{2\pi c}\frac{\exp(\mathrm{i}d_0\omega/c)}{\mathrm{i}d_0}\int_{-\infty}^{\infty}\tilde{U}_0(x_0,y_0,\omega) \times \mathrm{e}^{\mathrm{i}\frac{\omega}{2d_0c}\left[(x_1-x_0)^2+(y_1-y_0)^2\right]}\mathrm{d}x_0\mathrm{d}y_0\right\}\mathrm{e}^{-\mathrm{i}\omega t}\mathrm{d}\omega, \quad (5)$$

where

$$\tilde{U}_0(x_0,y_0,\omega) = \frac{1}{2\pi}\int_{-\infty}^{\infty}U_0(x_0,y_0,\tau)\,\mathrm{e}^{\mathrm{i}\omega\tau}\mathrm{d}\tau$$

is the Fourier transform of $U_0(x_0, y_0, \tau)$ and ω denotes the angular frequency. This indicates that the field amplitude of each point in plane (x_1, y_1) is the sum effect of all the frequency components. Because the diffraction fringe distributions of different monochromatic waves are different, the superposition of these diffraction fringes can lead to a smoothing effect on the far field according to the diffraction elimination condition

$$\mathrm{d}N_\mathrm{F} = -N_\mathrm{F}\frac{\mathrm{d}\lambda}{\lambda_0} > 0.5, \quad (6)$$

where N_F is the Fresnel number corresponding to the central wavelength λ_0, and $\mathrm{d}\lambda$ is the bandwidth of the incident pulsed beam. However, N_F is much less than one under practical circumstances. For example, the bandwidth should be about 3 μm to eliminate far-field diffraction for $a_0 = 250$ μm, $\lambda_0 = 1053$ nm and $d_1 = 0.1$ m. This is impractical for current practical pulsed lasers whose running bandwidth is less than several tens of nanometers. So the far-field diffraction fringe distribution of the pulsed beam can be viewed as almost the same as that of a corresponding monochromatic beam.

In the nonlinear medium (Kerr medium), the propagation is described in the retarded frame by the following generic nonlinear envelope equation[20]

$$\frac{\partial Q}{\partial \xi} = \frac{g_0}{2}Q + \mathrm{i}\frac{1}{2k_0}\left(1+\frac{\mathrm{i}}{\omega_0}\frac{\partial}{\partial\tau}\right)^{-1}\Delta_\perp Q - \mathrm{i}\frac{k''}{2}\frac{\partial^2 Q}{\partial\tau^2}$$

$$+ \mathrm{i}B_0 \left(1 + \frac{\mathrm{i}}{\omega_0}\frac{\partial}{\partial\tau}\right)|Q|^2 Q, \tag{7}$$

where Q denotes the electric field envelope which is normalized with A_0, ω_0 is the central angular frequency, $B_0 = k_0 P_0 n_2/n$ is the factor of nonlinear phase pushback per unit length, n_2 is the coefficient of nonlinear refractive index, P_0 is the peak power of the incident pulse, g_0 is the gain coefficient, $k'' = (\partial/\partial\omega)(1/V_g)|_{\omega=\omega_0}$ is the GVD coefficient, $\xi = z$ and $\Delta_\perp = \left(\partial^2/\partial x^2\right) + \left(\partial^2/\partial y^2\right)$. Note that here B_0 is not the B-integral which is a notion under the narrow-band condition. For the monochromatic beam case, the corresponding propagation equation in the nonlinear medium is

$$\frac{\partial Q}{\partial \xi} = \frac{g_0}{2}Q + \mathrm{i}\frac{1}{2k_0}\Delta_\perp Q + \mathrm{i}B_0|Q|^2 Q. \tag{8}$$

Comparing Eqs. (7) and (8), it can be expected that the time-dependent term will influence the results of the nonlinear image in pulsed beam. In Eq. (7), the operator $[1 + (\mathrm{i}/\omega_0)\,\partial/\partial\tau]$ approximates one if the pulse duration is longer than several tens of femtoseconds. In Refs. [9]–[13], authors assumed that the nonlinear medium was thin enough to make the change of energy distribution in the nonlinear medium neglectable. In practice, however, spatial distribution of energy was changed during propagation in nonlinear media , thereby leading to the difference between the thin slab-based theoretical prediction and the numerical results.[14] Moreover, the dispersion and the spatiotemporal coupling are also very important for the pulsed beam propagation, because they can influence the energy distribution in the pulsed beam and consequently the total nonlinear phase pushback through the nonlinear medium.

For the propagation in the free space II, again only diffraction takes effect and the pulse envelope can be obtained by the output envelope of the nonlinear medium with an expression similar to Eq. (5). Following the above analysis, bandwidth has an ignorable influence in this region as well.

Thus, it can be inferred that (i) the nonlinear medium thickness cannot be neglected for the pulsed beam case; (ii) nonlinear image may form under the illumination of pulsed beam but its intensity will be mainly dependent on spatiotemporal nonlinear interaction. In this paper, we refer to the peak intensity of the nonlinear image as the image intensity, which can reflect the threat to optical system caused by nonlinear images.

In what follows, we give the qualitative discussion based on the theory for the spatiotemporal interaction of the field in nonlinear mediums. The GVD term in Eq. (7) is related to three parameters: (i) the dispersion coefficient of the medium at the central frequency, (ii) the pulse duration, and (iii) the temporal uniformity of the complex envelope. When only the GVD effect is taken into account, the output temporal width of a Gaussian pulse for a nonlinear medium is[21]

$$\tau(L) = \left[\left(1 + \frac{Ck''L}{\tau_0^2}\right)^2 + \left(\frac{k''L}{\tau_0}\right)^2\right]^{1/2}\tau_0, \tag{9}$$

where L is the thickness of the nonlinear medium. Then, assuming that the nonlinear medium has normal GVD ($k'' > 0$), we discuss the formation of nonlinear image in pulsed laser beam through the following typical cases:

(i) incident pulses are transform-limited, i.e. $C = 0$. In this case, shorter pulses have broader bandwidth than longer ones. Behind the nonlinear medium, the pulse with smaller τ_0 has larger $\tau(L)$ and lower output peak intensity, indicating smaller nonlinear phase shift. So in this case the image intensity is proportional to τ_0.

(ii) incident pulses have the same durations but different values of C. In this case, the bandwidth of the incident beam increases as $|C|$ increases. For $C > 0$, from Eq. (9), the greater the value of C, the greater the degree of broadening by the nonlinear medium and thus the lower the image intensity. For $C < 0$, the pulsed beam will be temporally compressed at first in the nonlinear medium until the initial chirp is totally cancelled, which leads to a higher maximum intensity at the exit surface of the nonlinear medium than that in the case $C = 0$. Thus the image intensity will grow as $|C|$ increases. If $|C|$ is large enough, the image intensity can even be higher than that in the corresponding monochromatic beam case.

From the above analysis we can see that, for nonlinear mediums with normal GVD, the image intensity in pulsed beam without initial temporal chirp is lower than that in monochromatic beam, and that, if the incident pulse is temporally chirped, the intensity of nonlinear image can be higher or lower than that in the case without initial temporal chirp. However, because of the (3+1)-dimensional nature of the modulated pulsed beam, analytical solution of the propagation in the nonlinear medium and consequently that of the image intensity in pulsed beam are unfeasible in

mathematics till now, we will seek help from computer simulation as indicated in the following section.

4. Computer simulations

In this section, we numerically solve the imaging process by using the standard symmetric split-step Fourier algorithm. We use Eq. (7) as the model for simulation and set $g_0 = 0$ for simplicity. For free space, $k'' = 0$ and $B_0 = 0$. The step sizes in free space and nonlinear medium are 5 cm and 0.1 cm, respectively. Unless otherwise especially stated, in the following simulation and discussion, we assume that λ_0, τ_0, C and m are 800 nm, 0.25 ps, 0 and 4, respectively; for the scratch, a_0 and ρ are 250 μm and 0, respectively; d_o is 1 m; n_0, g_0, k'' and n_2 of the 10 cm Kerr medium are 1.45, 0, 3.6×10^{-26} s^2/m and 2.5×10^{-16} cm^2/GW at λ_0, respectively. Considering the thickness of the Kerr medium slab and the broadening effect in the Kerr medium, we set $B_0 \approx 23$. To characterize the imaging process, we define the maximum intensity of the pulse as $I_{\max} = |Q_{\max}(z)|^2$ and the central intensity as $I_c = |Q(0,0,z)|^2$. We note that, in what follows, when the effect of a parameter is discussed, other parameters not mentioned are kept unchanged. We first compare the imaging process with that in the monochromatic beam case, and then study how the bandwidth, the initial temporal chirp and the dispersion influence the nonlinear image respectively.

4.1. Main features of nonlinear image in pulsed laser beam

A comparison between the imaging process in the pulsed beam case and that in the monochromatic beam case is shown in Fig. 2. We can see from it the following similarities: (i) $\xi = 2.1$ m, which is the location of the so-called conjugate plane of the scatterer, is the position where $I_{\max}$ and I_c peak in both cases; (ii) the trends of the fluctuations of the peak and the central intensities in both cases are almost the same behind the nonlinear medium. These show that the nonlinear image of amplitude-type optical defect can also exist in the pulsed laser beam condition and its location is also at the conjugate position. However, the differences between these two cases are obvious. Firstly, the peak intensity of the nonlinear image in the pulsed beam case is evidently lower than that in the monochromatic beam case. Secondly, the peak intensity of the pulsed beam in the nonlinear medium grows more slowly than that of the monochromatic beam does. In addition, the curves almost overlap each other before the nonlinear medium, in accordance with the discussion about the influence of diffraction in the previous section. Figure 3 shows that the spatially central part of the pulsed beam intensity distribution at $\xi = 2.1$ m is approximately an inversion of that at $\xi = 0$ m and that the peak intensity at $\xi = 2.1$ m is very high.

Both Figs. 2 and 3 prove that nonlinear image can be formed in pulsed beam and its on-axis coordinate is almost the same as that in the monochromatic beam case, but the peak intensity of the nonlinear image is lower. This is in good agreement with the analysis in Section 3. In what follows, we refer to the on-axis coordinate where $I_{\max}$ and I_c simultaneously reach their maxima in free space II as the location of nonlinear image and define the corresponding peak intensity of pulsed beam as the image intensity $H_{\max}$.

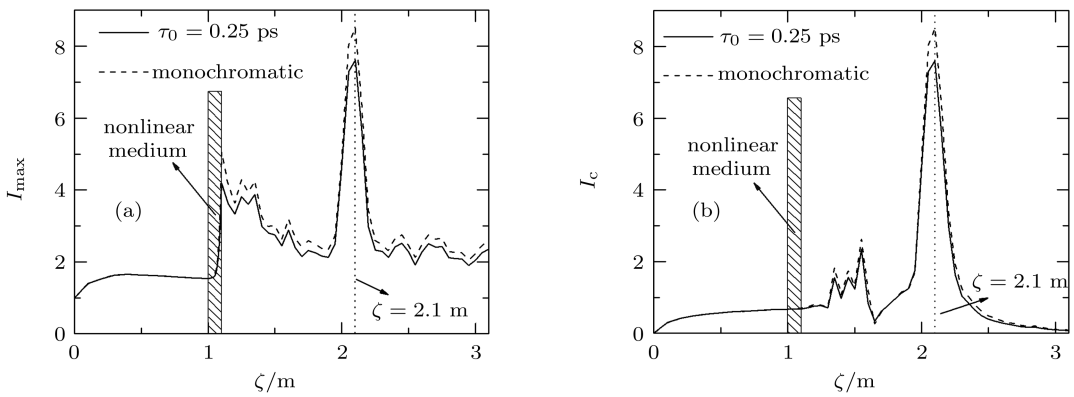


Fig. 2. Simulated evolutions of (a) $I_{\max}$ and (b) I_c of both pulsed beam (solid curves) and monochromatic beam (dash curves).

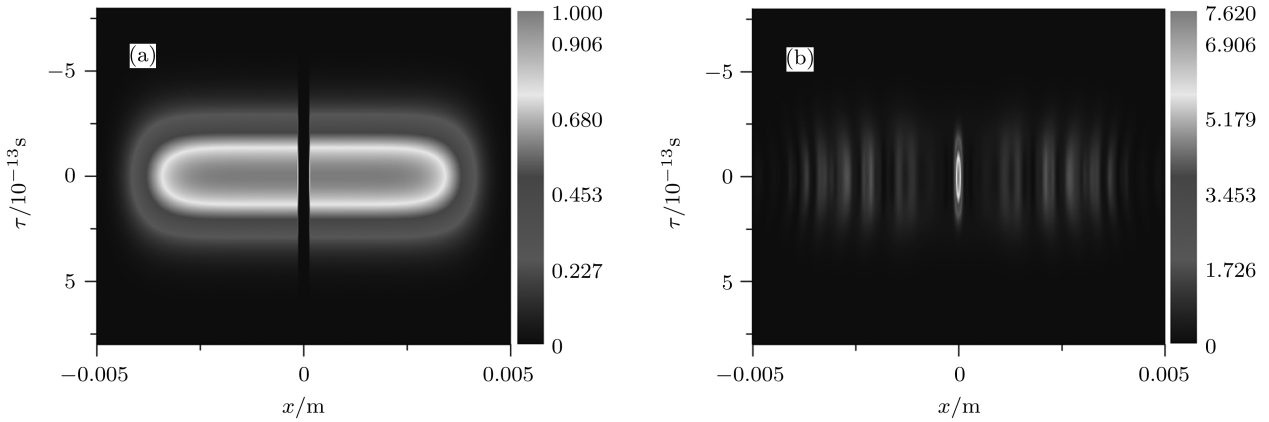


Fig. 3. Simulated normalized spatiotemporal distributions of the pulsed beam intensity in Fig. 2 at (a) $\xi = 0$ m and (b) $\xi = 2.1$ m.

4.2. Influence of chirp-type bandwidth on nonlinear image in pulsed beam

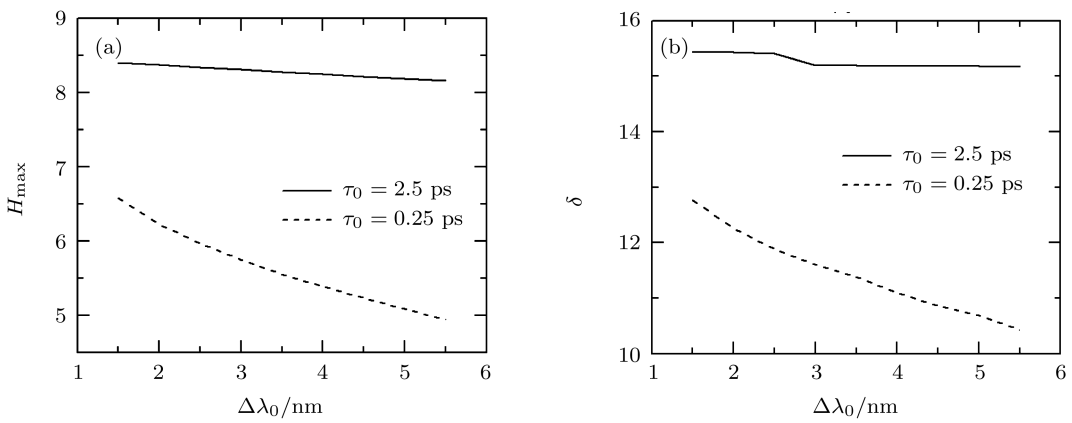
For incident Gaussian pulsed beam, the half width of the initial bandwidth is

$$\Delta\lambda = \sqrt{1 + C^2}\frac{\lambda_0}{\omega_0 \tau_0}. \tag{10}$$

So, for a certain τ_0, the same positive and negative temporal chirps correspond to the same initial bandwidth.

Figures 4(a) and 4(b) are the results for $C > 0$. In Fig. 4(a), the image intensity decreases as the bandwidth increases and is always lower than that in the corresponding monochromatic beam case (see the $I_{\max}$ at $\xi = 2.1$ m in Fig. 2). The slopes of both curves also become smaller as initial bandwidth increases. However, the curve corresponding to the smaller τ_0 changes more rapidly as bandwidth increases. For the contrast in the nonlinear image plane, which is defined as $\delta = I_{\max}/I_{\text{ave}}$, where I_{ave} is the average intensity at the position of nonlinear image, Fig. 4(b) shows that it also decreases as the initial bandwidth increases.

For incident pulses with $C < 0$, corresponding results are shown in Figs. 4(c) and 4(d). For $\tau_0 = 2.5$ ps, the image intensity is higher than that in the corresponding monochromatic beam case and is proportional to the bandwidth. For $\tau_0 = 0.25$ ps, when the bandwidth is relatively small, the image intensity is lower than that in the corresponding monochromatic beam case (see the $I_{\max}$ at $\xi = 2.1$ m in Fig. 2); as the bandwidth increases, the image intensity becomes higher and even higher than that in the corresponding monochromatic beam case and that in the longer pulse. Comparing Fig. 4(a) with Fig. 4(c), we can see that at a certain bandwidth point, the image intensity in the $C < 0$ case is always higher than that in the corresponding $C > 0$ case.



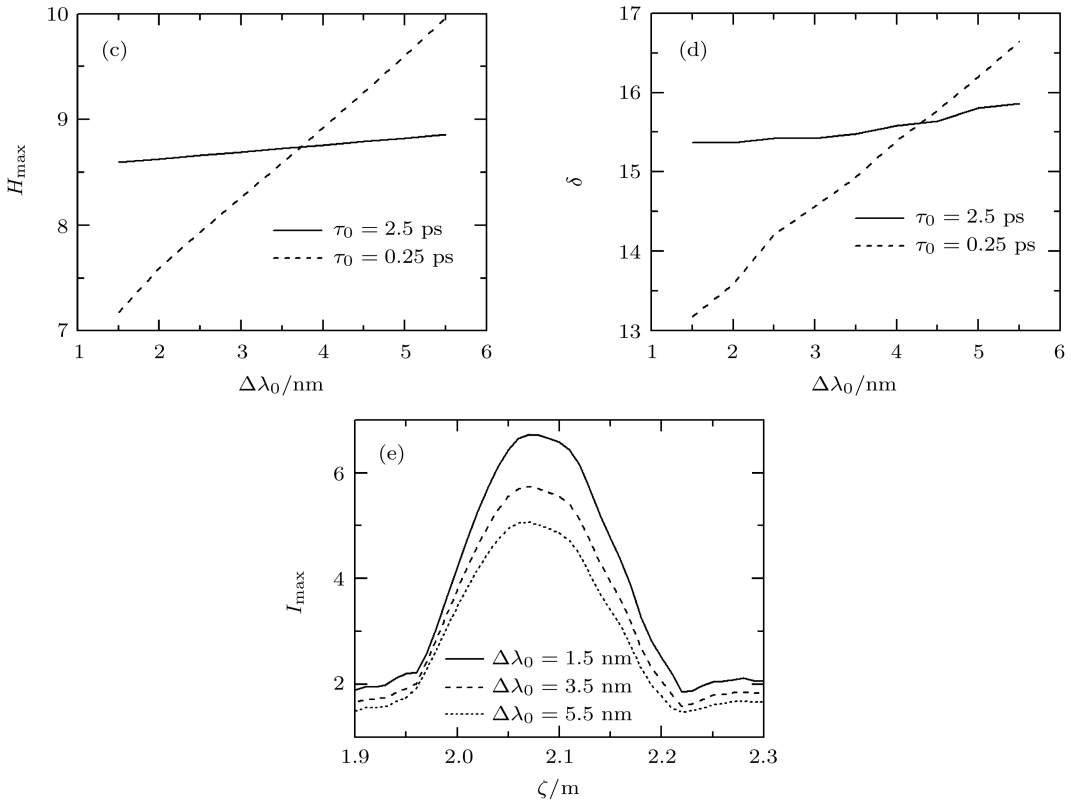


Fig. 4. (a) $H_{\max}$ and (b) δ versus $\Delta\ \lambda_0$ for $C > 0$. (c) and (d) are results for $C < 0$ corresponding to (a) and (b), respectively. (e) is the evolution of $I_{\max}$ around the conjugate location of the scatterer for $\tau_0 = 0.25$ ps and $C > 0$.

Figure 4(e) shows the evolution of $I_{\max}$ around the conjugate location of the scatterer. The step size of calculation is 1 cm. We can see from it that the top of the curve becomes lower as the incident bandwidth increases and that the top of the curve moves slightly toward the scratch. In a word, Fig. 4 shows that positive temporal chirp is helpful while negative temporal chirp is disadvantageous for suppressing nonlinear image, and, moreover, smaller pulse duration boosts these effects.

4.3. Influence of GVD effect on nonlinear image in pulsed beam

The GVD coefficient of the nonlinear medium can be positive or negative and its effect on pulse is related to the initial temporal chirp and the interplay with nonlinearity. For simplicity, we consider initially positive temporal chirp here. The simulation results are shown in Fig. 5. This figure clearly shows that, for the same incident pulsed beam, the image intensity decreases (increases) as the value of positive (negative) dispersion coefficient increases. This can be explained as follows: under normal GVD effect, the pulse is broadened after it has entred the medium, and the initially positive chirp of the pulse stimulates the broadening. So, as k'' increases, the nonlinear effect is weakened and thus the intensity of nonlinear image decreases; under anomalous GVD effect, because of the strong nonlinearity, the pulse is temporally compressed. So, as $|k''|$ increases, the nonlinear effect is enhanced and thus the intensity of nonlinear image increases.

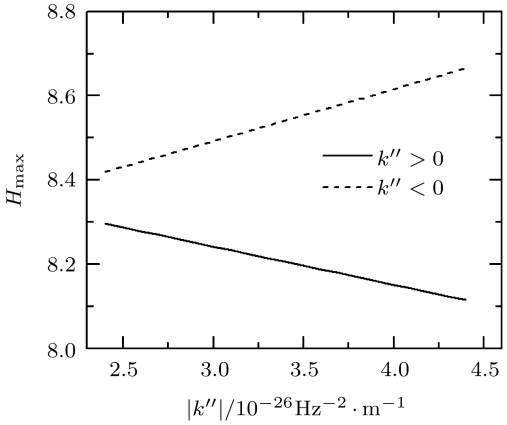


Fig. 5. Effect of GVD on image intensity. For the incident pulsed beam, $\Delta\lambda = 5$ nm and $\tau_0 = 2.5$ ps.

5. Conclusions

We have studied the formation of nonlinear image of amplitude-type scatterer in pulsed laser beam and the physical reasons for its differences from that in monochromatic beam. We have proved that nonlinear image can exist in pulsed beam and identified the influence of the bandwidth of incident pulsed beam and the GVD coefficient of nonlinear medium. When the GVD coefficient of the nonlinear medium is positive, the image intensity in transform-limited pulsed beam and that in pulsed beam with initially positive temporal chirp are found to be weaker, but that in pulsed beam with initially negative temporal chirp may be weak or intense compared with the nonlinear image in the monochromatic beam case. These effects are found to be enhanced as the bandwidth of the incident beam is increased by increasing initial temporal chirp or reducing initial pulse duration. Moreover, we also show that the GVD coefficient of nonlinear medium has an effect similar to chirp on nonlinear image. It can be predicted that the image intensity in pulsed beam tends to be as high as that in monochromatic beam if the duration of incident pulsed beam becomes big enough.

References

[1] Kelley P L 1965 *Phys. Rev. Lett.* **15** 1005

[2] Sun G Z, Ott E, Lee Y C and Guzdar P 1987 *Phys. Fluids* **30** 526

[3] Cao X D, Agrawal G P and McKinstrie J 1994 *Phys. Rev.* A **49** 4085

[4] Berkovsky A N, Kozlov S A and Shpolyanskiy Y A 2005 *Phys. Rev.* A **72** 043821

[5] Bespalov V I and Talanov V I 1966 *JETP Lett.* **3** 307

[6] Shen Y R 1975 *Prog. Quant. Electron.* **4** 1

[7] Campillo A J, Shapiro S L and Suydam B R 1973 *Appl. Phys. Lett.* **23** 628

[8] Wen S C, Qian L J and Fan D Y 2003 *Acta. Phys. Sin.* **52** 1640 (in Chinese)

[9] Hunt J T, Manes K R and Renard P A 1993 *Appl. Opt.* **32** 5973

[10] Widmayer C C, Milam D and de Szoeke S P 1997 *Appl. Opt.* **36** 9342

[11] Widmayer C C, Nickels M R and Milam D 1998 *Appl. Opt.* **37** 4801

[12] Xie L P, Jing F, Zhao J L, Su J Q, Wang W Y and Peng H S 2004 *Opt. Commun.* **236** 343

[13] Xie L P, Zhao J L and Jing F 2005 *Appl. Opt.* **44** 2553

[14] Peng T, Zhao J L, Xie L P, Yie Z J, Li Q and Su J Q 2007 *Acta. Phys. Sin.* **56** 3255 (in Chinese)

[15] Peng T, Zhao J L, Li D, Ye Z J and Xie L P 2009 *Chin. Phys.* B **18** 1884

[16] Wang Y W, Deng J Q, Wen S C, Tang Z X, Fu X Q and Fan D Y 2009 *Acta. Phys. Sin.* **58** 1738 (in Chinese)

[17] Skupsky S, Short R W, Kessler T, Craxton R S, Letzring S and Soures J M 1989 *J. Appl. Phys.* **66** 3456

[18] McKenty P W, Skupsky S, Kelly J H and Cotton C T 1994 *J. Appl. Phys.* **76** 2027

[19] Rothenberg J B 1997 *SPIE* **2633** 634

[20] Brabec T and Krausz F 1977 *Phys. Rev. Lett.* **78** 3282

[21] Agrawal G P 2001 *Nonlinear Fiber Optics* (New York: Academic) p70